
AGARD

ADVISORY GROUP FOR AEROSPACE RESEARCH & DEVELOPMENT

7 RUE ANCELLE 92200 NEUILLY SUR SEINE FRANCE

PROPAGATION MODELING OF MOIST AIR AND SUSPENDED
WATER/ICE PARTICLES AT FREQUENCIES BELOW 1000 GHz

H. J. Liebe
G. A. Hufford
M. G. Cotton

National Telecommunications and Information Administration
Institute for Telecommunication Sciences
325 Broadway, Boulder, CO 80303
U.S.A

**Paper Reprinted from
AGARD Conference Proceedings 542**

Atmospheric Propagation Effects through Natural and Man-Made Obscurants for Visible to MM-Wave Radiation

(Les Effets des Conditions Défavorables de
Propagation sur les Systèmes Optiques,
IR et à Ondes Millimétriques)

*Presented at the Electromagnetic Wave Propagation Panel Symposium,
held in Palma de Mallorca, Spain, 17th—20th May 1993.*



NORTH ATLANTIC TREATY ORGANIZATION

The Mission of AGARD

According to its Charter, the mission of AGARD is to bring together the leading personalities of the NATO nations in the fields of science and technology relating to aerospace for the following purposes:

- Recommending effective ways for the member nations to use their research and development capabilities for the common benefit of the NATO community;
- Providing scientific and technical advice and assistance to the Military Committee in the field of aerospace research and development (with particular regard to its military application);
- Continuously stimulating advances in the aerospace sciences relevant to strengthening the common defence posture;
- Improving the co-operation among member nations in aerospace research and development;
- Exchange of scientific and technical information;
- Providing assistance to member nations for the purpose of increasing their scientific and technical potential;
- Rendering scientific and technical assistance, as requested, to other NATO bodies and to member nations in connection with research and development problems in the aerospace field.

The highest authority within AGARD is the National Delegates Board consisting of officially appointed senior representatives from each member nation. The mission of AGARD is carried out through the Panels which are composed of experts appointed by the National Delegates, the Consultant and Exchange Programme and the Aerospace Applications Studies Programme. The results of AGARD work are reported to the member nations and the NATO Authorities through the AGARD series of publications of which this is one.

Participation in AGARD activities is by invitation only and is normally limited to citizens of the NATO nations.

REPORT DOCUMENTATION PAGE			
1. Recipient's Reference	2. Originator's Reference	3. Further Reference	4. Security Classification of Document
	AGARD-CP-542	ISBN 92-835-0727-4	UNCLASSIFIED/ UNLIMITED
5. Originator	Advisory Group for Aerospace Research and Development North Atlantic Treaty Organization 7 Rue Ancelle, 92200 Neuilly sur Seine, France		
6. Title	ATMOSPHERIC PROPAGATION EFFECTS THROUGH NATURAL AND MAN-MADE OBSCURANTS FOR VISIBLE TO MM-WAVE RADIATION		
7. Presented at	the Electromagnetic Wave Propagation Panel Symposium, held in Palma de Mallorca, Spain, 17th-20th May 1993.		
8. Author(s)/Editor(s)	Various		9. Date November 1993
10. Author's/Editor's Address	Various		11. Pages 208

14. Abstract
This publication reports the papers presented to a specialists' meeting held by the Electromagnetic Wave Propagation Panel at its Spring 1993 meeting.
The topics covered on the occasion of that Symposium include:
Natural obscurants:
— The effects of natural obscurants (haze, clouds, fog, rain, snow and dust) on system performance.
Man-made obscurants and battlefield-induced phenomena:
— The effects of man-made smokes, battlefield-induced smokes and enhanced scintillation on system performance.
Target and background signatures:
— Atmospheric effects on target and background signatures, and target to background contrast.
Multispectral camouflage:
— Weather-related propagation effects on camouflage and obscurants effectiveness and contrast reduction.
— Theoretical and/or experimental evaluation of camouflage effectiveness.
System mitigation aspects:
— Methods to mitigate the above-mentioned factors e.g. image processing, sensor fusion, tactical weather intelligence, and tactical decision aids.

Published November 1993

Copyright © AGARD 1993

All Rights Reserved

ISBN 92-835-0727-4



Printed by Specialised Printing Services Limited
40 Chigwell Lane, Loughton, Essex IG10 3TZ

PROPAGATION MODELING OF MOIST AIR AND SUSPENDED WATER/ICE PARTICLES AT FREQUENCIES BELOW 1000 GHz

H. J. Liebe
G. A. Hufford
M. G. Cotton

National Telecommunications and Information Administration
Institute for Telecommunication Sciences
325 Broadway, Boulder, CO 80303
U.S.A

SUMMARY

Propagation characteristics of the atmosphere are modeled for the frequency range from 1 to 1000 GHz (1 THz) by the modular millimeter-wave propagation model MPM. Refractivity spectra of the main natural absorbers (i.e., oxygen, water-vapor, suspended droplets and ice particles) are computed from known meteorological variables. The primary contributions of dry air come from 44 O₂ lines. Results from extensive 60-GHz laboratory measurements of the pressure-broadened O₂ spectrum were applied to update the line data base. The water-vapor module considers 34 local H₂O lines plus continuum contributions from the H₂O spectrum above 1 THz, which are formulated as wing response of a pseudo-line centered at 1.8 THz. Cloud/fog effects are treated with the Rayleigh approximation employing revised formulations for the permittivities of water and ice.

The influence of the Earth's magnetic field on O₂ absorption lines becomes noticeable at altitudes between 30 and 120 km. Anisotropic medium properties result, which are computed by the Zeeman propagation model ZPM. Here the elements of a complex refractivity tensor are determined in the vicinity (± 10 MHz) of O₂ line centers and their effect on the propagation of plane, polarized radiowaves is evaluated.

A spherically stratified (0 - 130 km) atmosphere provides the input for the codes MPM and ZPM in order to analyze transmission and emission properties of radio paths. Height profiles of air and water vapor densities and of the geocoded magnetic field are specified. ZPM predicts polarization- and direction-dependent propagation through the mesosphere. Emission spectra of the 9⁺ line (61150 \pm 3 MHz) for paths with tangential heights ranging from 30 to 125 km are consistent with data measured by the shuttle-based millimeter-wave limb sounder MAS.

1. INTRODUCTION

The natural atmospheric absorbers of oxygen, water vapor, and suspended water-droplets or ice-crystals, determine the propagation properties of the nonprecipitating atmosphere. The spectral characteristics of these absorbers are predicted up to 1000 GHz based on the physical conditions at altitudes from sea level to 130 km. Both phase and amplitude response of a plane radio wave propagating the distance z at frequency ν are described by a field strength,

$$E(z) = \exp[i k z (1 + N \times 10^{-6})] E(0),$$

where $E(0)$ is the initial value, $k = 2\pi\nu/c$ is the free space wave number, and c is the speed of light in vacuum. The spectral characteristics of the atmospheric medium are

expressed by a complex refractivity,

$$N = N_0 + N' + i N'' \quad \text{ppm} \quad (1)$$

The real part changes the propagation velocity (refraction) and consists of a frequency-independent term, N_0 , plus the dispersive refraction $N'(\nu)$. The imaginary part quantifies the loss of radiation energy (absorption). Refractivity N determines the specific quantities of power attenuation α and phase dispersion β or delay rate τ . Assuming frequency ν in GHz, one obtains

$$\begin{aligned} \alpha &= 0.1820 \nu N'' && \text{dB/km,} \\ \beta &= 1.2008 \nu (N_0 + N') && \text{deg/km,} \\ \tau &= 3.3356 (N_0 + N') && \text{ps/km.} \end{aligned}$$

Under special circumstances the refractivity N can exhibit *anisotropic* properties (e.g., mesospheric O₂ Zeeman effect). In such a case the propagation of plane, polarized waves is characterized by a two-dimensional field vector $E^T(z)$ which is affected perpendicular to the direction of propagation by a 2×2 refractivity matrix N .

2. ATMOSPHERIC REFRACTIVITY

2.1 Input Variables

Complex refractivity N is the central quantity computed by the Millimeter-wave Propagation Model MPM.^{1,2} Here, the opportunity is taken to update MPM89² with the latest spectroscopic information. The model considers 44 O₂ and 34 H₂O local lines (centered below 1000 GHz), nonresonant spectra for dry air, and an empirical water vapor continuum which reconciles experimental discrepancies. Model formulations for dry air and water vapor spectra follow closely the theory of absorption by atmospheric gases that is reviewed in detail by Rosenkranz.³ The refractivity of suspended water and ice particles is computed with the Rayleigh absorption approximation.⁴ Atmospheric conditions in MPM are characterized by the input variables:

		Typical Range
- barometric pressure	p	$10^5 - 1013$ mb
- ambient temperature	t	$-100 - 50$ °C
- relative humidity	u	$0 - 100$ %
- water droplet density	w	$0 - 5$ g/m ³
- ice particle density	w_i	$0 - 1$ g/m ³
- magnetic field strength	B	$20 - 65$ μ T.

For modeling purposes, a reciprocal temperature variable is introduced, $\theta = 300/(t + 273.15)$, and the barometric pressure p (1 mb = 100 Pa) is separated into partial pressures for dry air (p_d) and water vapor (e); i.e.,

$$p = p_d + e \quad \text{mb.}$$

2.2 Dry-Air Module

Refractivity of dry air is expressed by

$$N_D = N_d + \sum_k S_k F_k + N_n \quad \text{ppm}, \quad (2)$$

where the nondispersive term is

$$N_d = 0.2588 p_d \theta.$$

2.2.1 Oxygen Line Terms

The main contributions to N_D come from 44 O_2 spectral lines (k = line index). Each line strength,

$$S_k = (a_1 / \nu_k) p_d \theta^3 \exp [a_2 (1 - \theta)] \quad \text{ppm},$$

is multiplied by the complex shape function,

$$F(\nu) = \nu \left[\frac{1 - i\delta_k}{\nu_k - \nu - i\gamma_k} - \frac{1 + i\delta_k}{\nu_k + \nu + i\gamma_k} \right] \quad (3)$$

The Van Vleck-Weisskopf function $F(\nu)$ was modified by Rosenkranz³ to include line overlap effects. Width (γ) and overlap (δ) parameters of pressure-broadened O_2 lines in air are

$$\gamma_k = a_3 \times 10^{-3} (p_d \theta^{2.4} + 1.10 e \theta) \quad \text{GHz}$$

and

$$\delta_k = (a_5 + a_6 \theta) p \theta^{0.8}.$$

A rough estimate of line behavior in the mesosphere can be obtained by replacing γ_k with

$$\gamma_h = (\gamma_k^2 + 625 B^2)^{1/2},$$

where B is the magnetic field strength (22 - 65 μT) depending on the geographic location and altitude (see Sect. 2.3).

Extensive laboratory measurements of 60-GHz absorption by dry air have been reported recently.⁵ A best fit to these data established new coefficients a_5 and a_6 for the microwave lines. Still, the values listed for a_3 and $a_{5,6}$ in Table 1 are different from Ref. 5. Indirect evidence from the data suggests that all microwave widths γ_k are multiplied by 1.05.

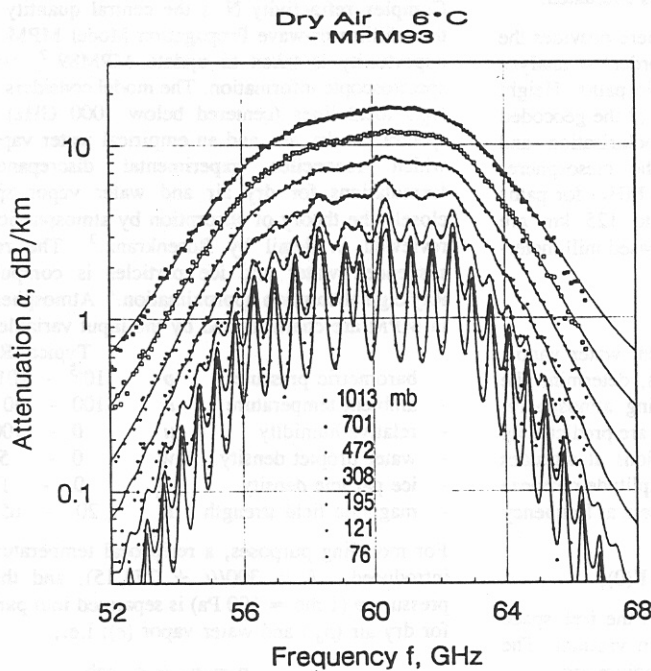


Figure 1. Dry air attenuation α from 52 to 68 GHz at 6°C for pressures from 1013 to 76 mb: MPM93 (lines), measured data⁵ (symbols).

This correction reduced on the average by 7 percent the rms error of the residuals for all 5400 data points when, in addition, the δ_k 's were raised by a factor of 1.15.⁵ Center frequencies ν_k and spectroscopic coefficients a_1 to a_6 are listed in Table 1.

The good fit between predicted attenuation rates and measured data points is illustrated in Fig. 1. Some of the very first attenuation rates (14 values, 49 - 59 GHz) for sea-level conditions were reported in 1956.⁶ These field-measured data agree well with predictions based on Eq. (2).

2.2.2 Nonresonant Terms

Nonresonant refractivity,

$$N_n = S_o F_o(\nu) + i S_n F_n''(\nu) \quad \text{ppm},$$

consists (a) of the nonresonant O_2 spectrum,

$$S_o = 6.14 \times 10^{-5} p_d \theta^2,$$

$$F_o = -\nu / (\nu + i\gamma_o),$$

where the relaxation frequency is $\gamma_o = 0.56 \times 10^{-3} p \theta^{0.8}$; and (b) of small contributions above 100 GHz by pressure-induced N_2 absorption,

$$S_n = 1.40 \times 10^{-12} p_d^2 \theta^{3.5},$$

$$F_n'' \approx \nu / (1 + 1.9 \times 10^{-5} \nu^{1.5}).$$

2.3 Zeeman-Effect of O_2 Lines

In the mesosphere, oxygen line absorption is complicated.⁷⁻⁹ Three separate complex-valued Zeeman refractivity patterns, $N_{\sigma^{\pm}}$ and N_{π} , are brought out by the geomagnetic field vector B^* . The refractivity that influences the field components of a plane wave is expressed in matrix form,⁸

$$N = \begin{bmatrix} N_{\pi} \sin^2 \phi + (N_{\sigma^+} + N_{\sigma^-}) \cos^2 \phi & -i(N_{\sigma^+} - N_{\sigma^-}) \cos \phi \\ i(N_{\sigma^+} + N_{\sigma^-}) \cos \phi & N_{\sigma^+} + N_{\sigma^-} \end{bmatrix}$$

where ϕ is the angle between the direction of propagation and the magnetic vector B^* . The refractivity elements of an isolated line are represented by

$$N_{\sigma^{\pm}, \pi} = N_d + S_k \sum_M \xi_M F_M \quad \text{ppm}, \quad (4)$$

where ξ_M is a relative strength factor defined in such a way that the sum of the Zeeman components equals the strength value (a_1) of the unsplit ($B = 0$) line. The center frequency of individual lines within a pattern is determined by

$$\nu_M = \nu_k + 28.03 \times 10^{-6} \eta_M B \quad \text{GHz},$$

where the relative shift factor η_M lies between +1 and -1. The index M stands for the azimuthal quantum number M , which controls the structure of a Zeeman pattern.⁹ The scheme for determining ξ_M and η_M hinges on the quantum number identification of a particular O_2 line and can be found in Refs. 8, 9. The correct shape function is a Voigt profile,³ which was approximated by a Lorentzian profile,

$$F_M = \nu / (\nu_M - \nu - i\gamma_h),$$

where the transition to Doppler-broadening at $h \geq 50$ km ($p \leq 0.8$ mb) is given for each Zeeman component by

$$\gamma_h = 0.535 \gamma_k + (0.217 \gamma_k^2 + \gamma_D^2)^{1/2} \quad \text{GHz}.$$

The Doppler width is $\gamma_D = 1.096 \times 10^{-6} \nu_M \theta^{1/2}$.

2.4 Water-Vapor Module

The MPM-input for water vapor is relative humidity u , which is converted to vapor pressure $e = (u/100) e_s$ by way of the saturation pressure e_s over water (or ice)¹⁰ at temperature t . A useful approximation for saturation over water is given by

$$e_s = 2.408 \times 10^{11} \theta^{5.5} \exp(-22.644 \theta) \text{ mb.}$$

Absolute humidity (water-vapor density) follows from

$$q = 0.7223 e \theta \text{ g/m}^3.$$

Refractivity of atmospheric water vapor is written in the form

$$N_V = N_V + \sum_t S_t F_t + N_c \text{ ppm,} \quad (5)$$

where the nondispersive term is

$$N_V = (4.163 \theta + 0.239) e \theta.$$

2.4.1 H₂O Line Spectrum

Line refractivity results from 34 local H₂O resonances (ℓ = line index). The individual line strength is

$$S_\ell = (b_1 / \nu_\ell) e \theta^{3.5} \exp[b_2(1 - \theta)] \text{ ppm;}$$

the shape function is that of Eq. (3). The width of a pressure-broadened H₂O line is formulated by¹¹

$$\gamma_\ell = b_3 \times 10^{-3} (b_4 e \theta^{b_6} + p_d \theta^{b_5}) \text{ GHz.}$$

Line overlap is neglected ($\delta_\ell = 0$) and Doppler-broadening is approximated for pressures below 0.7 mb ($h \geq 60$ km) by

$$\gamma_\ell^* = 0.535 \gamma_\ell + (0.217 \gamma_\ell^2 + \gamma_D^2)^{1/2},$$

where the Doppler width is $\gamma_D = 1.46 \times 10^{-6} \nu_\ell \theta^{-1/2}$.

2.4.2 H₂O Continuum Spectrum

The contributions of local lines in Eq. (5) are not sufficient to match measured data. In particular, absorption data in the window ranges between spectral lines reflect a magnitude up to five times larger than predicted values. The excess is taken into account by a continuum spectrum N_c , which originates in the strong lines centered in the rotational H₂O spectrum above 1 THz.^{14, 20} Absolute absorption data from controlled experiments^{15 - 19} provide the basis for formulating a physical model of N_c . Pure water vapor and foreign-gas (air or N₂) mixtures were studied at 18 - 40 GHz¹⁵, 138 GHz¹⁶, 186 - 194 GHz¹⁷, 213.5 GHz¹⁸, and 160 - 920 GHz¹⁹.

At 137.8 GHz, pressure and temperature dependences of moist air absorption data were fitted with 10% rms to¹⁶

$$N_c'' = e (k_s e + k_f p_d) 10^{-6} \nu \text{ ppm,} \quad (6)$$

where $k_s = 0.357 \theta^{7.5}$ and $k_f = 0.0113 \theta^3$. This equation was then applied to define the continuum for MPM89.²

At 213.5 GHz, new absorption data of moist nitrogen have been reported,¹⁸ which fitted with an oxygen-free MPM exceptionally well to Eq. (6):

$$k_s = 0.444 \theta^{7.5} \quad (0.4\% \text{ rms}) \text{ and}$$

$$k_f = 0.0145 \theta^{4.5} \quad (1.0\% \text{ rms}).$$

Similar data closer to the 183-GHz line center¹⁷ yielded initially a fitting error of 14.6% rms, which improved to 4.5% rms when the theoretical¹² strength value b_1 was increased by 5 percent. A theoretical approximation of the real part,²⁰

$$N_c' \approx e \theta^{2.5} 0.791 \times 10^{-6} \nu^2 \text{ ppm,}$$

was also considered in the fitting exercise.

An analytical match of the continuum was considered by means of a *pseudo*-line centered out-of-band above 1 THz. Expanding the line shape, Eq. (3), into a power series and assuming that $\delta = 0$, $\gamma_c \ll \nu_c$, and $\nu \rightarrow 0$, leads to:

$$N_c'' \approx 2 S_c \gamma_c [(\nu/\nu_c) + 3 (\nu/\nu_c)^3] \nu_c^{-2} \text{ and} \quad (7)$$

$$N_c' \approx 2 S_c [(\nu/\nu_c)^2 + (\nu/\nu_c)^4] \nu_c^{-1}$$

Different fits to Eq. (7) resulted in three sets of parameters for this pseudo-line:

ν_c	b_1	b_2	b_3	b_4	b_5	b_6	Data Ref.
GHz	kHz/mb		MHz/mb				
2200	4210	0.952	17.8	30.5	2	5	15, 18, 19
1780	2230	0.952	17.6	30.5	2	5	15, 18, Table 2
1470	1257	0.952	17.3	30.5	2	5	15, 18, 20

For the "continuum" line N_c centered at $\nu_c = 1780$ GHz and the chosen units one can assert that

$$k_s (\theta = 1) = 2 \times 10^3 b_1 b_3 b_4 \nu_c^{-3} = 0.434 \text{ GHz}^{-1} \text{ mb}^{-2},$$

which is close to the value found by fitting the 213.5-GHz data alone (see above). The second-order ν -terms of Eq. (7) allow one to "tailor" the fit close to the upper frequency limit of MPM (1 THz) by changing ν_c . An exact fit to both measured absorption data¹⁹ and analytical refraction results²⁰ around 900 GHz was not possible. Hence, the continuum line parameters ν_c and b_1 in Table 2 are a compromise which is of no consequence to data fits below about 800 GHz. Both the large widths for far-wing self- $(b_3 \times b_4)$ and air-broadening (b_3) and the strong negative temperature dependence (b_6) have been postulated by theory.^{14, 21}

Table 2 lists the present line frequencies ν_ℓ and spectroscopic coefficients b_1 to b_6 (ν_ℓ and b_1 are from Ref. 12). The b_1 values of the 22-GHz line* and 183-GHz¹⁷ lines were increased by 5 percent to fit measured data.

The MPM for moist air is made up by $N = N_D + N_V$. Predictions of N'' are compared with published data in Figs. 2 to 4. The critical temperature dependence of N_c'' is represented in Fig. 2. The frequency dependence of three data sets^{15, 17-19} is shown in Figs. 3 and 4. Measured data in Fig. 4 span a range from 160 to 920 GHz.¹⁹ MPM-predicted attenuation rates $\alpha(\nu)$ are plotted in Fig. 5 for sea-level conditions (100% RH) at five temperatures ($\pm 40^\circ\text{C}$).

2.5 Cloud/Fog Module

The interaction of suspended water droplets and ice crystals with radio waves is treated by employing the Rayleigh approximation for Mie extinction,

$$N_W = 1.5 (w/m_{w,i}) [(\epsilon_{w,i} - 1)(\epsilon_{w,i} + 2)^{-1}], \quad (8)$$

where $m_{w,i} = 1$ and $0.916 \text{ (g/cm}^3\text{)}$ are specific weights, and $\epsilon_{w,i}$ complex permittivities of water and ice, respectively.⁴ For the size spectra ($r \leq 50 \mu\text{m}$) of suspended water droplets, Eq. (8) is valid up to about 300 GHz. Fog or cloud conditions are specified by a water mass density w . Water droplets form when the relative humidity exceeds saturation, $u = 100 - 101$ percent, whereby t can be as low as -40°C (supercooled state). Propagation effects caused by ice crystals (needles and plates) are primarily depolarizing and scattering in nature.

* The increase in the b_1 -coefficient for the 22.2-GHz line was suggested by ground-level emission measurements.¹³ Data at 20.6 GHz exhibited a systematic trend which was not apparent in 31.7- and 90-GHz data taken simultaneously. On-site radiosonde recordings of height profiles for p , t , and u furnished independent input to test three prediction models.

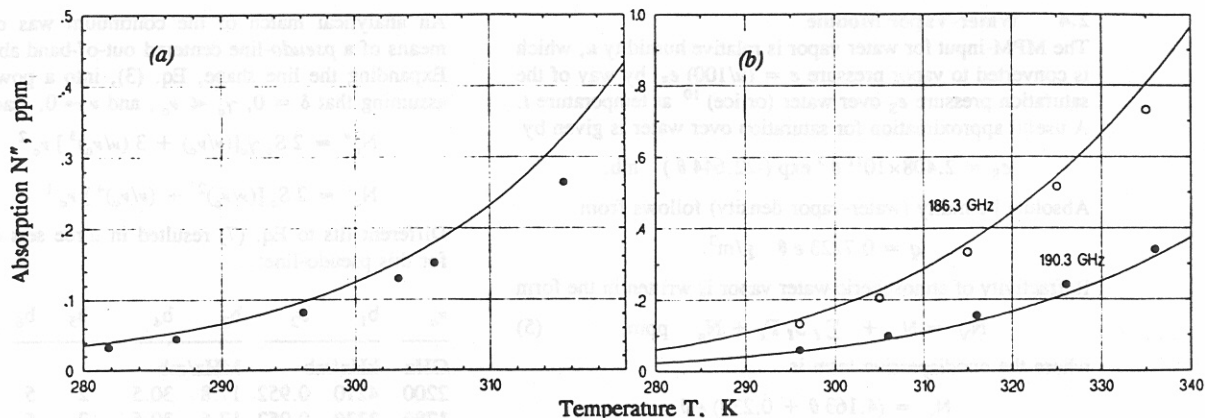


Figure 2. Absorption data N'' versus temperature T in kelvin: (a) moist air at 137.8 GHz ($p = 1013$ mb, $u = 80\%$)¹⁶, and (b) mixture of water vapor and nitrogen (186.3 and 190.3 GHz, $p = 1000$ mb, $u = 10\%$)¹⁷. — MPM93.

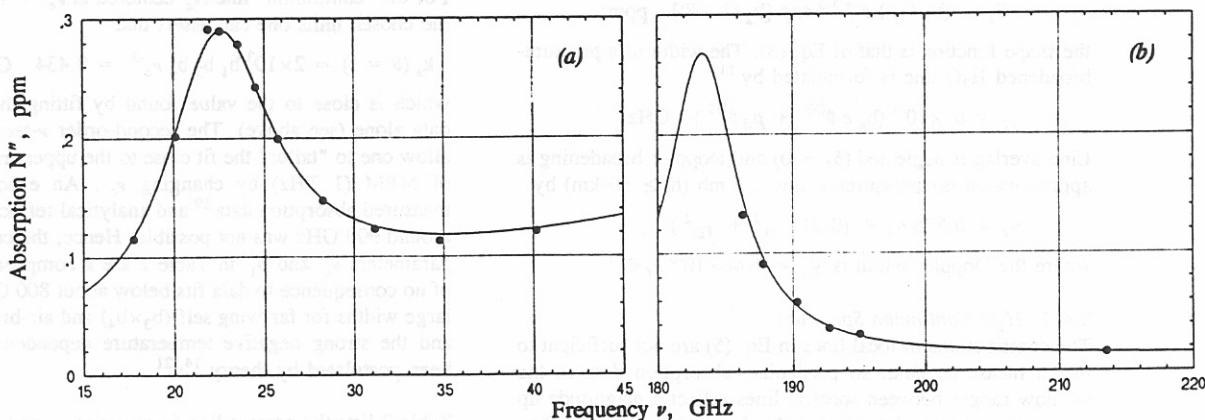


Figure 3. Absorption data N'' over two frequency ranges: (a) moist air (318 K, $p = 1013$ mb, $u = 80\%$)¹⁵, and (b) mixture of water vapor and nitrogen (296 K, $p = 1000$ mb, $u = 10\%$)^{17,18}. — MPM93.

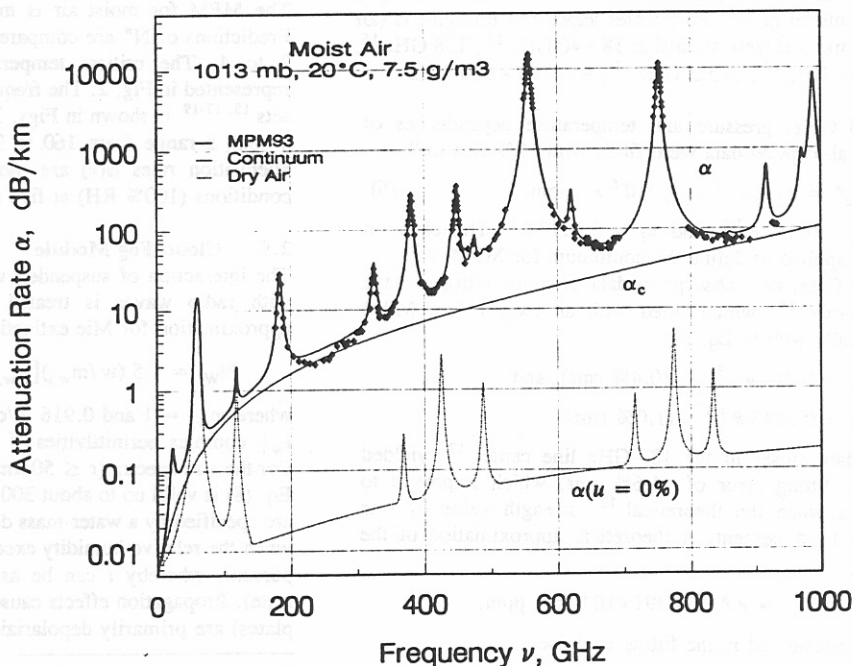


Figure 4. Attenuation rate α and continuum of moist air ($u = 43.4\%$) and of dry air ($u = 0\%$) as predicted by MPM93 for standard sea-level conditions ($p = 1013$ mb, $t = 20^\circ\text{C}$). Data points are from Ref. 19.

TABLE 1. Spectroscopic Coefficients of O₂ Lines in Air

Center Freq. ν_k	Strength		Width		Overlap	
	a_1	a_2	a_3^*	a_4	a_5^*	a_6^*
GHz	kHz/mb		MHz/mb		10^3 /mb	
50.474238	9.400E-08	9.694	0.89	0.8	0.240	0.790
50.987749	2.460E-07	8.694	0.91	0.8	0.220	0.780
51.503330	6.080E-07	7.744	0.94	0.8	0.197	0.774
52.021410	1.414E-06	6.844	0.97	0.8	0.166	0.764
52.542394	3.102E-06	6.004	0.99	0.8	0.136	0.751
53.066907	6.410E-06	5.224	1.02	0.8	0.131	0.714
53.595749	1.247E-05	4.484	1.05	0.8	0.230	0.584
54.130000	2.280E-05	3.814	1.07	0.8	0.335	0.431
54.671159	3.918E-05	3.194	1.10	0.8	0.374	0.305
55.221367	6.316E-05	2.624	1.13	0.8	0.258	0.339
55.783802	9.535E-05	2.119	1.17	0.8	-0.166	0.705
56.363389	1.344E-04	1.660	1.20	0.8	0.390	-0.113
56.968206	1.763E-04	1.260	1.24	0.8	-0.297	0.753
57.612484	2.141E-04	0.915	1.28	0.8	-0.416	0.742
58.323877	2.386E-04	0.626	1.33	0.8	-0.613	0.697
58.446590	1.457E-04	0.084	1.52	0.8	-0.205	0.051
59.164207	2.404E-04	0.391	1.39	0.8	0.748	-0.146
59.590983	2.112E-04	0.212	1.43	0.8	-0.722	0.266
60.306061	2.124E-04	0.212	1.45	0.8	0.765	-0.090
60.434776	2.461E-04	0.391	1.45	0.8	-0.705	0.081
61.150560	2.504E-04	0.626	1.36	0.8	0.697	-0.324
61.800154	2.298E-04	0.915	1.31	0.8	0.104	-0.067
62.411215	1.933E-04	1.260	1.27	0.8	0.570	-0.761
62.486260	1.517E-04	0.083	1.23	0.8	0.360	-0.777
62.997977	1.503E-04	1.665	1.54	0.8	-0.498	0.097
63.568518	1.087E-04	2.115	1.20	0.8	0.239	-0.768
64.127767	7.335E-05	2.620	1.17	0.8	0.108	-0.706
64.678903	4.635E-05	3.195	1.13	0.8	-0.311	-0.332
65.224071	2.748E-05	3.815	1.10	0.8	-0.421	-0.298
65.764772	1.530E-05	4.485	1.07	0.8	-0.375	-0.423
66.302091	8.009E-06	5.225	1.05	0.8	-0.267	-0.575
66.836830	3.946E-06	6.005	1.02	0.8	-0.168	-0.700
67.369598	1.832E-06	6.845	0.99	0.8	-0.169	-0.735
67.900867	8.010E-07	7.745	0.97	0.8	-0.200	-0.744
68.431005	3.300E-07	8.695	0.94	0.8	-0.228	-0.753
68.960311	1.280E-07	9.695	0.92	0.8	-0.240	-0.760
118.750343	9.450E-05	0.009	0.90	0.8	-0.250	-0.765
368.498350	6.790E-06	0.049	1.63	0.8	-0.036	0.009
424.763124	6.380E-05	0.044	1.92	0.2	0	0
487.249370	2.350E-05	0.049	1.93	0.2	0	0
715.393150	9.960E-06	0.145	1.92	0.2	0	0
773.839675	6.710E-05	0.130	1.81	0.2	0	0
834.145330	1.800E-05	0.147	1.82	0.2	0	0

TABLE 2. Spectroscopic Coefficients of H₂O Lines in Air

Center Freq. ν_k	Strength		Width				
	b_1^*	b_2	b_3	b_4	b_5	b_6	
GHz	kHz/mb		MHz/mb				
22.235080	0.01130 ⁺	2.143	2.811	4.80	0.69	1.00	
67.803960	0.00012	8.735	2.858	4.93	0.69	0.82	
119.995940	0.00008	8.356	2.948	4.78	0.70	0.79	
183.310091	0.24200 ⁺	0.668	3.050 ⁺	5.30	0.64	0.85	
321.225644	0.00483	6.181	2.303	4.69	0.67	0.54	
325.152919	0.14990	1.540	2.783	4.85	0.68	0.74	
336.222601	0.00011	9.829	2.693	4.74	0.69	0.61	
380.197372	1.15200	1.048	2.873	5.38	0.54 ⁺	0.89 ⁺	
390.134508	0.00046	7.350	2.152	4.81	0.63	0.55	
437.346667	0.00650	5.050	1.845	4.23	0.60	0.48	
439.150812	0.09218	3.596	2.100	4.29	0.63	0.52	
443.018295	0.01976	5.050	1.860	4.23	0.60	0.50	
448.001075	1.03200	1.405	2.632	4.84	0.66	0.67	
470.888947	0.03297	3.599	2.152	4.57	0.66	0.65	
474.689127	0.12620	2.381	2.355	4.65	0.65	0.64	
488.491133	0.02520	2.853	2.602	5.04	0.69	0.72	
503.568532	0.00390	6.733	1.612	3.98	0.61	0.43	
504.482692	0.00130	6.733	1.612	4.01	0.61	0.45	
547.676440 [*]	0.97010	0.114	2.600	4.50	0.70	1.00	
552.020960 [*]	1.47700	0.114	2.600	4.50	0.70	1.00	
556.936002	48.74000	0.159	3.210	4.11	0.69	1.00	
620.700807	0.50120	2.200	2.438	4.68	0.71	0.68	
645.866155 [*]	0.00713	8.580	1.800	4.00	0.60	0.50	
658.005280	0.03022	7.820	3.210	4.14	0.69	1.00	
752.033227	23.96000	0.396	3.060	4.09	0.68	0.84	
841.083973	0.00140	8.180	1.590	5.76	0.33	0.45	
859.962313	0.01472	7.989	3.060	4.09	0.68	0.84	
899.306675	0.00605	7.917	2.985	4.53	0.68	0.90	
902.616173	0.00426	8.432	2.865	5.10	0.70	0.95	
906.207325	0.01876	5.111	2.408	4.70	0.70	0.53	
916.171582	0.83410	1.442	2.670	4.78	0.70	0.78	
923.118427 [*]	0.00869	10.22	2.900	5.00	0.70	0.80	
970.315022	0.89720	1.920	2.550	4.94	0.64	0.67	
987.926764	13.21000	0.258	2.985	4.55	0.68	0.90	
1780 [*]	2230	0.952	17.6	30.5	2	5	

*Different from MPM89 2

+Based on measured data